Theoretical Study of Gas-Phase Reactions of $Fe(CO)_5$ with OH^- and Their Relevance for the Water Gas Shift Reaction

Maricel Torrent,[†] Miquel Solà,*[,†] and Gernot Frenking*[,‡]

Institut de Química Computacional, Campus de Montilivi, Universitat de Girona, E-17071 Girona, Spain, and Fachbereich Chemie, Philipps-Universität Marburg, Hans-Meerwein-Strasse, D-35032 Marburg, Germany

Received December 28, 1998

Revision of the homogeneously $Fe(CO)_5$-catalyzed water gas shift reaction in the gas phase has been performed by means of quantum chemical calculations using gradient-corrected density functional theory (B3LYP) and ab initio methods at the CCSD(T) level. The classically assumed reaction path has been scrutinized step by step, and enlarged with novel mechanistic proposals. Our calculations lend additional credit to some of the previously accepted steps in the catalytic cycle, such as the initial attack of OH^- to $Fe(CO)_5$ and also to the recently accepted decarboxylation of $(CO)_4FeCOOH^-$ (via a concerted mechanism involving a four-centered transition state), as well as to the acidification of the metal hydride $(CO)_4FeH^-$ with water to yield the dihydride $(CO)_4FeH_2$. The present investigation also examines in terms of energies and activation barriers the existence/participation of new intermediates (in particular, a metalloformate species, a water−hydride adduct, and a dihydrogen complex), not mentioned in prior studies. Finally, a transition-metal-containing S_N2-type reaction is explored for the last stages of this chemical process as a mechanistic alternative to regenerate the starting catalyst.

Introduction

The water gas shift reaction (WGSR), eq 1, is a key process in the worldwide chemical industry.[1] Its importance derives from its role both as a means for enriching the H_2 content of water gas (synthesis gas) and as a side reaction of significance in hydroformylation and Fischer−Tropsch processes.[2] In manufacturing practice, the WGSR is promoted by heterogeneous catalysts at high temperature and pressure. However, several homogeneous systems exist that require less severe conditions.[3] Investigations have shown that reaction 1 can be carried out at considerably lower temperatures with water present as a liquid by using homogeneous catalysts to accelerate the reaction.[4]

$$CO(g) + H_2O(g) \rightarrow H_2(g) + CO_2(g) \qquad (1)$$

Homogeneous catalysis of the WGSR by transition-metal (TM) carbonyls has received considerable attention since the first examples were reported some 50 years ago.[5] Because of the formation of CO_2, one obvious requirement for a TM carbonyl to be a catalyst of practical value for the above reaction is that it must be capable of generating a metal hydride species through attack by a base. The base must be weak enough so that it can be regenerated from its carbonate salt upon moderate heating. Several TM carbonyls have been studied;[6,7] however, among mononuclear metal carbonyls, only $Fe(CO)_5$ and $Ru(CO)_5$ appear to meet this requirement.[8,9]

The $Fe(CO)_5$-catalyzed WGSR was initially proposed[9] to proceed via the cycle displayed in Scheme 1. The

[†] Universitat de Girona.
[‡] Philipps-Universität Marburg.

(1) (a) Lukehart, C. M. *Fundamental Transition Metal Organometallic Chemistry*; Geoffroy, G. L., Ed.; Brooks/Cole Publishing: CA, 1985, Chapter 13. (b) Collman, J. P., Hegedus, L. S., Norton, J. R., Finke, R. G., Eds. *Principles and Applications of Organotransition Metal Chemistry*; University Science Books: Mill Valley, CA, 1987. (c) Wilkinson, S. G., Gillard, R. D., McCleverty, J. A., Eds. *Comprehensive Coordination Chemistry: The Synthesis, Reactions, Properties & Applications of Coordination Compounds*; Pergamon: Oxford, England, 1987; Vol. 6, pp 269−292.

(2) (a) Storch, H. H.; Golumbic, N.; Anderson, R. B. *The Fischer−Tropsch and Related Syntheses*; Wiley: New York, 1951. (b) *Catalyst Handbook*; Springer-Verlag: London, 1970; Chapters 5 and 6. (c) Keim, W., Ed. *Catalysis in C_1 Chemistry*; D. Reidel Publishing Co.: Dordrecht, The Netherlands, 1983; pp 50 and 136. (d) Shelef, M.; Gandhi, H. S. *Ind. Eng. Chem., Prod. Res. Dev.* **1975**, *13*, 80. (e) Querido, R.; Short, W. L. *Ind. Eng. Chem., Process Des. Dev.* **1973**, *12*, 10. (f) Lin, G. I.; Samokhin, P. V.; Kaloshkin, S. D.; Rozovskii, A. Y. *Kinet. Catal.* **1998**, *39*, 577.

(3) Ford, P. C. *Acc. Chem. Res.* **1981**, *14*, 31 and references therein.

(4) (a) Yoshida, T.; Ueda, Y.; Otsuka, S. *J. Am. Chem. Soc.* **1978**, *100*, 3942. (b) Laine, R. M.; Thomas, D. W.; Carry, L. W.; Buttrill, S. E. *J. Am. Chem. Soc.* **1978**, *100*, 6527. (c) Ford, P. C.; Rinker, R. G.; Laine, R. M.; Ungermann, C.; Landis, V.; Moya, S. A. *Adv. Chem. Ser.* **1979**, *173*, 81. (d) Ungermann, C.; Landis, V.; Moya, S. A.; Cohen, H.; Walker, H.; Pearson, R. G.; Ford, P. C. *J. Am. Chem. Soc.* **1979**, *101*, 5922. (e) Baker, E. C.; Hendriksen, D. E.; Eisenberg, R. *J. Am. Chem. Soc.* **1980**, *102*, 1020. (f) King, A. D.; King, R. B.; Yang, D. B. *Chem. Commun.* **1980**, 529.

(5) (a) Reppe, J. W.; Reindl, E. *Liebigs Ann. Chem.* **1953**, *582*, 121. (b) Frazier, C. C.; Hanes, R. B.; King, A. D.; King, R. B. *Adv. Chem. Ser.* **1979**, *173*, 94. (c) Darensbourg, D. J.; Darensbourg, M. Y.; Burch, R. R.; Froelich, J. A.; Incorvia, M. J. *Adv. Chem. Ser.* **1979**, *173*, 106. (d) Yoshida, T.; Thorn, D. L.; Okano, T.; Ibers, J. A.; Otsuka, S. *J. Am. Chem. Soc.* **1979**, *101*, 4212.

10.1021/om9810504 CCC: $18.00
Publication on Web 06/29/1999

Scheme 1. Initially Proposed Mechanism for the WGSR Catalysis Using Iron Pentacarbonyl

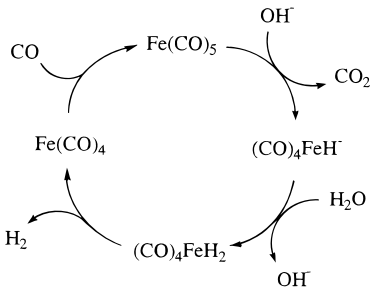

reactions shown in this scheme do not necessarily represent actual steps in the catalysis. In fact, some of the original steps have been redefined in more detail because of further investigations.[10,11] An improved approach to the catalytic cycle could be formulated as follows:

$$Fe(CO)_5 + OH^- \rightarrow (CO)_4FeCOOH^- \quad (2)$$

$$(CO)_4FeCOOH^- \rightarrow (CO)_4FeH^- + CO_2 \quad (3)$$

$$(CO)_4FeH^- + H_2O \rightarrow (CO)_4FeH_2 + OH^- \quad (4)$$

$$(CO)_4FeH_2 \rightarrow H_2 + Fe(CO)_4 \quad (5)$$

$$Fe(CO)_4 + CO \rightarrow Fe(CO)_5 \quad (6)$$

Therefore, the $Fe(CO)_5$-catalyzed process is nowadays believed to involve nucleophilic activation of CO followed by decarboxylation of the transient metallocarboxylic acid $(CO)_4FeCOOH^-$ to form CO_2 and the metal hydride $(CO)_4FeH^-$. Formation of the conjugate acid of the hydride, i.e., $(CO)_4FeH_2$, is believed to precede evolution of H_2. Then, $Fe(CO)_4$ which is also liberated reacts with CO to regenerate the starting complex, thus completing the catalytic cycle.

Support has been provided for most of steps 2−6 taken as individual reactions. Nucleophilic attack of a metal-bonded carbonyl group by OH^- to give a metal-bonded carboxyl group (eq 2) is now well-established in metal carbonyl cation chemistry[12,13] and has reasonable experimental support in the rhodium carbonyl catalyzed WGSR.[7] Carboxyl groups directly bonded to TMs similar to that in the proposed intermediate $(CO)_4FeCOOH^-$ are well-known to undergo facile decarboxylation to give the corresponding metal hydride,[13,14] as in eq 3. Finally, $(CO)_4FeH_2$ is known to be a weak acid[15] and a powerful catalyst for double-bond isomerization reactions.[16] Moreover, it is found to decompose readily with liberation of molecular hydrogen[17] as in eq 5. Most of these reactions, however, have been reported to proceed either in solution or under conditions which are different from the ones in the catalytic cycle.

Very recently, experimental data from a gas-phase ion study combined with other thermochemistry have been reported by Sunderlin and Squires[18] in order to derive a model reaction energy profile for the title chemical process. Their investigation is interesting for comparison to solution-phase results. It was found[18] that, in the gas phase, the initial step of addition of OH^- to $Fe(CO)_5$ (eq 2) is highly exothermic whereas, in solution, this step is slower because OH^- is more effectively solvated than the bulkier $(CO)_4FeCOOH^-$, where the negative charge is more delocalized. Both decarboxylation and decarbonylation of $(CO)_4FeCOOH^-$ have similar barriers and endothermicities.[18] In solution, decarboxylation is found to be generally rapid (eq 3), suggesting that the barrier for decarboxylation is lowered by solvation.[18] Next, proton transfer from water to $(CO)_4FeH^-$ (eq 4) was found to be highly endothermic in the gas phase,[18] since $(CO)_4FeH_2$ is a strong acid. The reaction rate was reported to be slow in basic solutions[18] as previously predicted. Finally, loss of H_2 followed by addition of CO to reform $Fe(CO)_5$ (eqs 5 and 6) was found to be exothermic in the gas phase and rapid in solution.[18]

While much understanding of the catalytic cycle has been achieved, mechanistic details remain still unclarified largely due to difficulties in identifying and characterizing most of the transient intermediate species which are believed to be involved. In some cases, only indirect evidence exists that the postulated reactions should occur in the sequence in eqs 2−6 given above since these steps have only been studied individually, i.e., as single reactions. A complete picture of the catalytic cycle including both kinetical and thermodynamical data is necessary to determine the validity of the suggested mechanism for the WGSR catalysis. Once the kinetics and thermodynamics of such individual steps are characterized, it should be possible to predict conditions under which the proposed scheme would operate optimally.

To the best of our knowledge, a complete mechanistic study for this catalytic reaction has not been reported yet. Recent advances in computer technology and computational chemistry[19] have enabled a significant advance in the field of chemical reactivity for TM systems. Quantum chemical calculations are also used now to gain insight into the mechanisms of homogeneous

(6) Laine, R. M.; Rinker, R. S.; Ford, P. C. *J. Am. Chem. Soc.* **1977**, *99*, 253.
(7) (a) Cheng, C.-H.; Hendricksen, D. E.; Eisenberg, R. *J. Am. Chem. Soc.* **1977**, *99*, 2791. (b) Kubiak, C. P.; Eisenberg, R. *J. Am. Chem. Soc.* **1980**, *102*, 3637. (c) Kubiak, C. P.; Woodcock, C.; Eisenberg, R. *Inorg. Chem.* **1982**, *21*, 1, 2119. (d) Tominaga, K.; Sasaki, Y.; Hagihara, K.; Watanabe, T.; Saito, M. *Chem. Lett.* **1994**, 1391. (e) Kallinen, K. O.; Pakkanen, T. T.; Pakkanen, T. A. *J. Organomet. Chem.* **1997**, *547*, 319. (f) Bryce, D. J. F.; Dyson, P. J.; Nicholson, B. K.; Parker, D. G. *Polyhedron* **1998**, *17*, 2899. (g) Clark, R. J. H.; Dyson, P. J.; Humphrey, D. G.; Johnson, B. F. G. *Polyhedron* **1998**, *17*, 2985.
(8) Gross, D. C.; Ford, P. C. *Inorg. Chem.* **1982**, *21*, 1704.
(9) Kang, H.; Mauldin, C.; Cole, T.; Slegeir, W.; Petit, R. *J. Am. Chem. Soc.* **1977**, *99*, 8323.
(10) Grice, N.; Kao, S. C.; Pettit, R. *J. Am. Chem. Soc.* **1979**, *101*, 1627.
(11) Lane, K. R.; Lee, R. E.; Sallans, L.; Squires, R. R. *J. Am. Chem. Soc.* **1984**, *106*, 5767.
(12) Kruck, T.; Noack, M. *Chem. Ber.* **1964**, *97*, 1693.
(13) Darensbourg, D. J.; Froelich, J. A. *J. Am. Chem. Soc.* **1977**, *99*, 4726.
(14) (a) Hieber, W.; Kruck, T. *Z. Naturforsch. B* **1961**, *16*, 709. (b) Clark, H. C.; Dixon, K. R.; Jacobs, W. J. *Chem. Commun.* **1968**, 548.
(15) Krumholz, P.; Stettiner, H. M. A. *J. Am. Chem. Soc.* **1949**, *71*, 3035.
(16) Sternberg, H. W.; Markby, R.; Wender, I. *J. Am. Chem. Soc.* **1957**, *79*, 6116.
(17) Hieber, W.; Vetter, H. *Z. Anorg. Allg. Chem.* **1933**, *212*, 145.
(18) Sunderlin, L. S.; Squires, R. R. *J. Am. Chem. Soc.* **1993**, *115*, 337.
(19) (a) Ziegler, T. *Chem. Rev.* **1991**, *91*, 651. (b) Stevens, W. J.; Krauss, M.; Basch, H.; Jasien, P. G. *Can. J. Chem.* **1992**, *70*, 612.

Table 1. Calculated and Experimental Reaction Energies ΔE (kcal mol^{-1}) for the Postulated Steps 2−6 and Other Related Reactions Involved in the Catalytic Cycle,[a,b] with Numbering of the Species as in Scheme 2

reaction	ΔE(B3LYP/II)			ΔE(B3LYP/II)			ΔE(CCSD(T)/II++)			exptl
$CO + H_2O \rightarrow CO_2 + H_2$	−19.0	(−21.9)	*−24.9*	−11.3	(−14.2)	*−17.2*	−3.7	(−6.6)	*−9.6*	−9.8[c]
$Fe(CO)_5$ (**1**) + OH^- → $(CO)_4FeCOOH^-$ (**2a**)	−106.5	(−101.8)	*−97.8*	−70.5	(−65.8)	*−61.8*	−71.1	(−66.4)	*−62.4*	−60.8 ± 3.4[d]
$(CO)_4FeCOOH^-$ (**2a**) → $(CO)_4FeOCOH^-$ (**2b**)	−3.4	(−4.4)	*−5.0*	−3.4	(−4.4)	*−5.0*				
$(CO)_4FeCOOH^-$ (**2a**) → $(CO)_4FeH^-$ (**3**) + CO_2	−5.2	(−8.6)	*−12.5*	−3.9	(−7.3)	*−11.2*	6.4	(3.0)	*−0.9*	−4 ± 7[d]
$(CO)_4FeH^-$ (**3**) + H_2O → $(CO)_4FeH^-{\cdot}H_2O$ (**4**)	−8.5	(−6.9)	*−4.8*	−7.0	(−5.4)	*−3.3*				
$(CO)_4FeH^-{\cdot}H_2O$ (**4**) → $(CO)_4FeH_2$ (**5**) + OH^-	115.9	(111.8)	*106.9*	82.6	(78.5)	*73.6*				
$(CO)_4FeH^-$ (**3**) + H_2O → $(CO)_4FeH_2$ (**5**) + OH^-	107.4	(104.9)	*102.1*	75.6	(73.1)	*70.3*	71.9	(69.4)	*66.6*	71.5[d]
$(CO)_4FeH_2$ (**5**) → $(CO)_4FeH_2$ (**6**)	8.4	(8.2)	*8.3*	7.9	(7.7)	*7.8*	12.0	(11.8)	*11.9*	
$(CO)_4FeH_2$ (**6**) → $Fe(CO)_4$ (**7**) + H_2	17.1	(12.8)	*9.7*	17.5	(13.2)	*10.1*	24.4	(20.1)	*17.0*	
$(CO)_4FeH_2$ (**5**) → $Fe(CO)_4$ (**7**) + H_2	25.5	(21.0)	*18.0*	25.4	(20.9)	*17.9*	36.4	(31.9)	*28.9*	26 ± 2[e]
$Fe(CO)_4$ (**7**) + CO → $Fe(CO)_5$ (**1**)	−40.2	(−37.4)	*−34.7*	−37.9	(−35.1)	*−32.4*	−47.3	(−44.5)	*−41.9*	−41.5[f]

[a] Numbers in parentheses include the ZPE correction computed at B3LYP/II. [b] Numbers in italics include ZPE + thermal corrections computed at B3LYP/II. [c] Reference 34. [d] Reference 18. [e] Reference 38. [f] Reference 72.

Table 2. Imaginary Frequencies[a] (in cm^{-1}), and Calculated and Experimental Activation Barriers[b,c] (kcal mol^{-1}) for Some Selected Steps, with Numbering of the Species as in Scheme 2

TS	$\nu^{\ddagger}$	$E^{\ddagger}$(B3LYP/II)			$E^{\ddagger}$(B3LYP/II++)			$E^{\ddagger}$(CCSD(T)/II++)			exptl
TS(**2a** → **3**)	1456*i*	33.6	(29.3)	*24.8*	33.7	(29.4)	*24.9*	33.8	(29.5)	*25.0*	18.9 ± 3[d]
TS(**5** → **6**)	735*i*	9.0	(8.6)	*6.2*	8.6	(8.2)	*5.8*				

[a] Computed at B3LYP/II. [b] Numbers in parentheses include the ZPE correction computed at B3LYP/II. [c] Numbers in italics include ZPE + thermal corrections computed at B3LYP/II. [d] Reference 18.

catalysis.[20] It is our goal to shed light on the mechanism of the $Fe(CO)_5$-catalyzed WGSR by taking advantage of these recent advances in theoretical chemistry. There are many intriguing questions to be asked about this reaction for which computational chemistry might give an answer. In particular, regarding the intermediates of the postulated cycle, do all of them play an active role in the reaction mechanism? Are other species involved? If so, what are their molecular and electronic structures? And which are the transition states (TSs) or short-lived intermediates connecting them? Most importantly, what type of reactions does each intermediate itself undergo, and what are the kinetics and energetics of these processes? Overall, the work described herein is concerned with a critical reassessment of the entire mechanism. Comparison with experimental data has been also made whenever possible.

Methods

The geometry optimizations have been carried out at the DFT level using the three-parameter fit of the exchange-correlation potential suggested by Becke (B3LYP).[21] Two different basis sets (II and II++) have been used in this study. Basis set II uses a small-core effective core potential (ECP) with a (441/2111/41) split-valence basis set for Fe, which is derived from the (55/5/5) minimal basis set optimized by Hay and Wadt,[22] and 6-31G(d,p) all-electron basis sets[23] for C, O, and H. The performance of basis set II has been systematically studied for calculating TM compounds somewhere else.[24] Basis set II++ is the same as II plus the addition of an s diffuse function on H and a set of three sp diffuse functions on C and O atoms. Here the use of diffuse functions turned out to be crucial because some of the active species involved in the catalytic cycle are anions. Single-point energy calculations of B3LYP/II-optimized structures have been performed (i) at B3LYP/II++, and (ii) using coupled-cluster theory with singles and doubles and noniterative estimation of triple excitations,[25] CCSD(T)/II++. The nature of the stationary points has been investigated by calculating the Hessian matrices at the B3LYP/II level. Vibrational frequencies reveal that all structures reported have the correct number of negative eigenvalues (zero for minima and one for transition states). Gaussian94[26] has been employed for the DFT calculations. The CCSD(T) calculations have been done with the program Molpro.[27]

Results and Discussion

Thermochemical data regarding steps 2−6 and other related reactions relevant for a complete description of the catalytic cycle are collected in Table 1. Table 2 summarizes the kinetic information for the most critical steps. The numbering of the complexes has been indicated in Scheme 2 where the symmetry of each species is also given. As seen from Scheme 2, the most relevant new features are as follows: (i) investigation of a metalloformate complex, **2b**, besides the metallocarboxylic acid **2a**, (ii) elucidation of the decarboxylation process **2a** → **3** + CO_2 followed by acidification of hydride **3** with H_2O to yield species **5**, (iii) analysis of the dichotomy between dihydride **5** and an unprec-

(20) *Theoretical Aspects of Homogeneous Catalysis*; van Leuwen, P. W. N. M., Morokuma, K., van Lenthe, J. H., Eds.; Kluwer Academic Publishers: Dordrecht, The Netherlands, 1995.
(21) Becke, A. D. *J. Chem. Phys.* **1993**, *98*, 5648.
(22) Hay, P. J.; Wadt, W. R. *J. Chem. Phys.* **1985**, *82*, 299.
(23) (a) Ditchfield, R.; Hehre, W. J.; Pople, J. A. *J. Chem. Phys.* **1971**, *54*, 724. (b) Hehre, W. J.; Ditchfield, R.; Pople, J. A. *J. Chem. Phys.* **1972**, *56*, 2257. (c) Hariharan, P. C.; Pople, J. A. *Mol. Phys.* **1974**, *27*, 209. (d) Hariharan, P. C.; Pople, J. A. *Theor. Chim. Acta* **1973**, *28*, 213. (e) Gordon, M. S. *Chem. Phys. Lett.* **1980**, *76*, 163.
(24) Frenking, G.; Antes, I.; Böhme, M.; Dapprich, S.; Ehlers, A. W.; Jonas, V.; Neuhaus, A.; Otto, M.; Stegmann, R.; Veldkamp, A.; Vyboishchikov, S. F. In *Reviews in Computational Chemistry*; Lipkowitz, K. B., Boyd, D. B., Eds.; VCH: New York, 1996; Vol. 8, pp 63−144.
(25) (a) Pople, J. A.; Krishnan, R.; Schlegel, H. B.; Binkley, J. S. *Int. J. Quantum Chem.* **1978**, *14*, 545. (b) Barlet, R. J.; Purvis, G. D. *Int. J. Quantum Chem.* **1978**, *14*, 561. (c) Purvis, G. D.; Barlett, R. J. *J. Chem. Phys.* **1982**, *76*, 1910. (d) Purvis, G. D.; Barlett, R. J. *J. Chem. Phys.* **1987**, *86*, 7041.
(26) Frisch, M. J.; Trucks, G. W.; Schlegel, H. B.; Gill, P. M. W.; Johnson, B. G.; Robb, M. A.; Cheeseman, J. R.; Keith, T. A.; Petersson, G. A.; Montgomery, J. A.; Raghavachari, K.; Al-Laham, M. A.; Zakrewski, V. G.; Ortiz, J. V.; Foresman, J. B.; Cioslowski, J.; Stefanov, B. B.; Nanayakkara, A.; Challacombe, M.; Peng, C. Y.; Ayala, P. Y.; Chen. W.; Wong, M. W.; Andres, J. L.; Replogle, E. S.; Gomberts, R.; Martin, R. L.; Fox, D. J.; Binkley, J. S.; Defrees, D. J.; Baker, I.; Stewart, J. J. P.; Head-Gordon, M.; Gonzalez, C.; Pople, J. A. *Gaussian94*; Gaussian Inc.: Pittsburgh, PA, 1995.
(27) Werner, H.-J.; Knowles, P. J. Universität Stuttgart and University of Birmingham.

Scheme 2. New Proposed Scheme for the Mechanism of the $Fe(CO)_5$-Catalyzed WGSR Derived from the Present Study

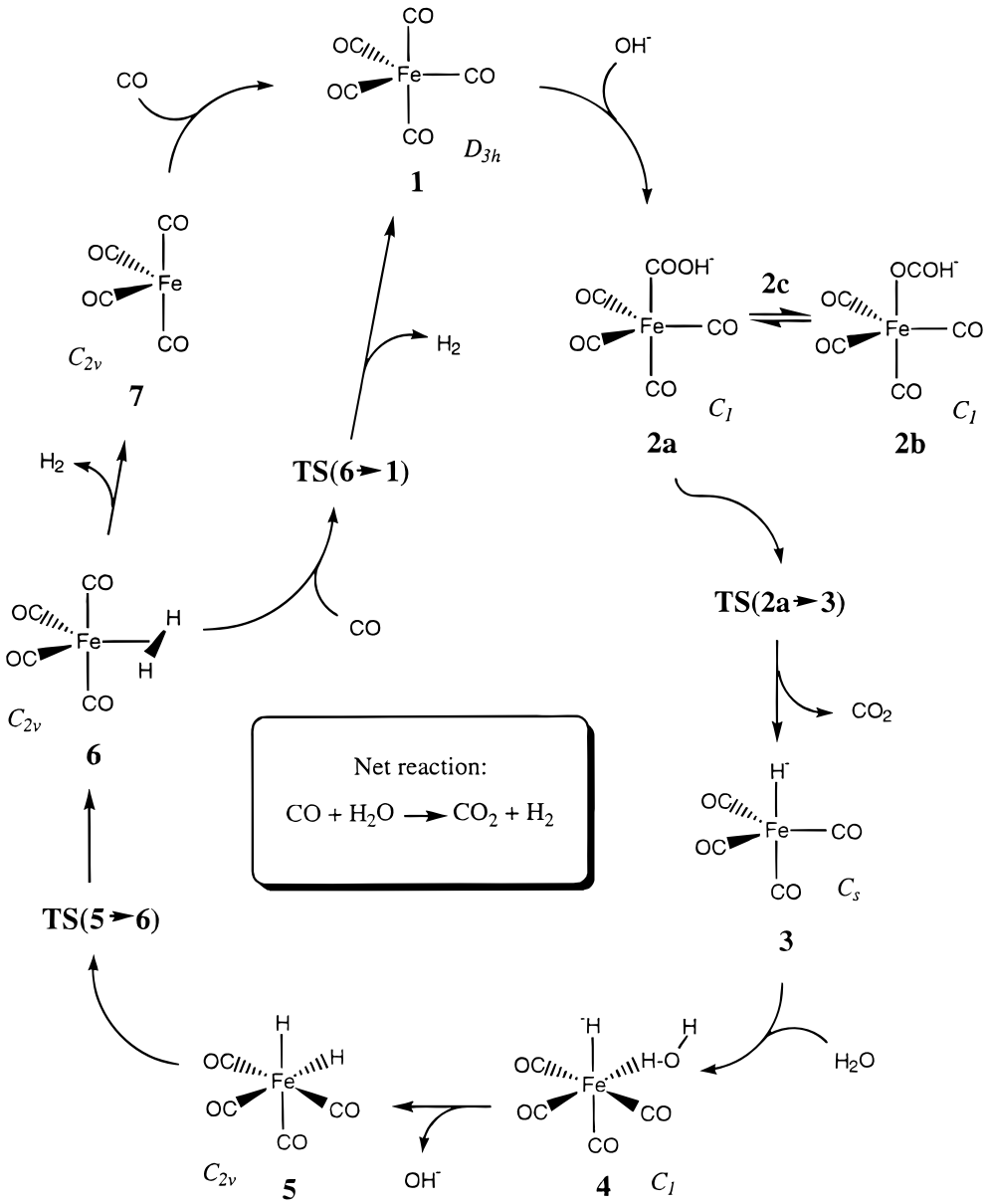

edented dihydrogen complex **6**, and (iv) exploration of an alternative path, **6** → **1**, to the classical route involving **7**. The results presented below are analyzed following Scheme 2.

The theoretically predicted geometry of **1** at the B3LYP/II level has Fe−CO bonds in excellent agreement (Fe−C_{ax} = 1.818 Å; Fe−C_{eq} = 1.805 Å) with the latest experimental data available (Fe−C_{ax} = 1.811(2) Å; Fe−C_{eq} = 1.803(2) Å).[28] The calculated C−O distances (C−O_{ax} = 1.147 Å; C−O_{eq} = 1.151 Å) are slightly longer than the ones observed (C−O_{ax} = 1.117(2) Å; C−O_{eq} = 1.133(3) Å),[28] but the differences between theoretical and experimental values are within the typical range of error at this level of theory (<0.03 Å). Our calculations predict that the axial Fe−C bond (1.818 Å) is longer than the equatorial Fe−C bond (1.805 Å). The question about the relative bond lengths of the axial and equatorial Fe−CO bonds has not definitely been answered yet.[29] In a pioneering gas-phase electron diffraction study[30] the average Fe−CO_{eq} distance (1.827 Å) was reported to be longer than the axial value Fe−CO_{ax} (1.807 Å). A recent X-ray diffraction analysis of the low-temperature crystals[28] showed that the equatorial Fe−CO bonds are slightly shorter (1.803 Å) than the axial Fe−CO bonds (1.811 Å). From the vibrational spectra and force constants of $Fe(CO)_5$, it had already been concluded that the equatorial Fe−CO bonds should be shorter than the axial Fe−CO bonds.[31] Previous calculations at the MCPF level of theory also predicted that the axial Fe−CO bonds should be longer than the equatorial bonds.[32] The opposite result, however, had been obtained at the CCI level.[33] Despite the still conflicting results, our calculations are consistent with

(28) Braga, D.; Grepioni, F.; Orpen, A. G. *Organometallics* **1993**, *12*, 1481.

(29) Ehlers, A. W.; Frenking, G. *Organometallics* **1995**, *14*, 423.
(30) Beagley, B.; Schmidling, D. G. *J. Mol. Struct.* **1974**, *22*, 466.
(31) Jones, L. H.; McDowell, R. S.; Goldblatt, M.; Swanson, B. I. *J. Chem. Phys.* **1972**, *57*, 2050.
(32) Barnes, L. A.; Rosi, M.; Bauschlicher, C. W., Jr. *J. Chem. Phys.* **1991**, *94*, 2031.

the most recent experimental source.[28] This can be taken as a measure of reliability for the method employed here, at least for the purpose of characterizing molecular structures.

To assess the validity of the present methodology for the purpose of evaluating also the reaction energies in the cycle, we can take as an approximate benchmark the reaction enthalpy of eq 1. Neither the metal system nor charged species are included in such a reaction; nevertheless, this benchmark is still useful to evaluate the methods herein employed. The enthalpy of reaction 1at 298 K is known[34] to be -9.8 kcal mol^{-1}. The theoretical value computed for this reaction using basis set II (-24.9 kcal mol^{-1}, Table 1) is clearly larger than the experimental value.[34] Hence, although basis set II is suitable to reproduce geometries, it does not seem reliable enough to evaluate reaction energies. A better estimate is obtained by employing basis set II++. The addition of diffuse functions reduces the difference between the theoretical predictions and the experimental value significantly (Table 1). This notwithstanding, the exothermicity of the reaction at B3LYP/II++ is still overestimated by 7.4 kcal mol^{-1}. The best prediction comes from the calculations performed at the CCSD(T)/II++ level, which only deviate 0.2 kcal mol^{-1} from the experimental result.

Coupled-cluster calculations are very expensive, and thus, it is not always possible to report them, especially when large systems are involved. In the following we report single-point calculations at the CCSD(T) level only for selected (mostly non-C_1) stationary points. In the steps involving C_1 complexes, the best estimate for the energetics is provided by B3LYP/II++ (see Table 1). It will be seen, however, that the B3LYP/II++ values do not substantially deviate from CCSD(T)/II++.

1. Nucleophilic Activation. Once the validity of the methods has been assessed, then we can turn to discussing the catalytic cycle step by step. Let us consider first the nucleophilic activation of a CO ligand in **1**. A linear transit calculation reveals that, in the early stages of the reaction, i.e., at long distances, the direction of attack of OH^- is approximately equidistant from the axial and the equatorial carbonyl ligands in **1** which seem therefore to play the same role. The initial approach is controlled by forces of electrostatic nature arising from both ligands. The last stage of the reaction, on the contrary, is controlled by molecular orbital type interactions. A slight preference for the attack of the axial carbonyl ligand is found. This may be traced, in part, to the fact that there is no empty d metal orbital pointing toward the equatorial ligand in $Fe(CO)_5$, and, in part, to the empty π^*_{CO} orbital being lower in energy for the axial carbonyl ligand, therefore inducing a greater stabilization when interacting with the lone pair orbital of the nucleophilic oxygen atom. The last stage of the reaction is essentially characterized by a bending of the attacked carbonyl ligand, which allows an approach of the hydroxyl at about 120° of the Fe−C bond. The advantages of this bending have been discussed elsewhere.[35]

As seen from Table 1, the addition of OH^- to **1** is highly exothermic, the computed exothermicity being -61.8 kcal mol^{-1}. We also found that, when the OH^- ion is initially located at ca. 5 Å far from the metal center, the system evolves toward the acid **2a** without formation of any adduct of the type $(CO)_5Fe\cdots OH^-$ or any other intermediate. This is an indication of a barrierless process. The experimental value[18] for reaction 2 has been recently reported to be -60.8 ± 3.4 kcal mol^{-1}, which is in very good agreement with our calculated data. The present results are also in agreement with previous works by Dedieu and Nakamura,[35,36] where a computed SCF reaction energy of -71.3 kcal mol^{-1} for the same nucleophilic addition[35] and of -69.2 kcal mol^{-1} for the nucleophilic addition[36] of H^- were reported. These authors also examined the reaction path for hydride addition and found likewise there was no barrier.[36]

Since nucleophiles are employed as cocatalysts in a variety of metal carbonyl catalyzed reactions, nucleophilic activation of coordinated CO holds considerable interest.[9,37] Despite it, there have been few detailed quantitative studies of such a common step in catalysis.[38,39] Besides the works mentioned above,[36,35] one of the most relevant studies may be that by Trautman et al.,[40] who examined the kinetics of CH_3O^- and OH^- addition to $Fe(CO)_5$ to give the corresponding adducts. Methoxide proved to be a more powerful nucleophile than hydroxyde under comparable conditions. The methoxycarbonyl adduct was found to be stable but the hydroxycarbonyl analogue underwent decarboxylation to give the metal hydride anion $(CO)_4FeH^-$,[40] which is in fact the next reaction step of the WGSR.

2. Metallocarboxylic Acid vs Metalloformate Complex. Before discussing the decarboxylation process, we draw attention to species **2a** and related compounds. The only species reported so far to be a plausible intermediate deriving from the nucleophilic addition of OH^- to **1** has been the organometallic anion $(CO)_4FeCOOH^-$.[11] In contrast, the homogeneous WGSR catalysis by group 6 metals has been recently found to involve formate complexes[41−44] analogous to surface-bound formates observed in heterogeneous WGSR.[45] For instance, the chromium formate complex, $(CO)_5CrO_2CH^-$, loses CO_2 to form $(CO)_5CrH^-$, whereas the tungsten formate, $(CO)_5WO_2CH^-$, may be isolated and decarboxylates very slowly.[42,46] Although metal formates have not been generally regarded as key intermediates in

(33) Lüthi, H. P.; Siegbahn, P. E. M.; Almlöf, J. *J. Phys. Chem.* **1985**, *89*, 2156.
(34) King, A. D. Jr.; King, R. B.; Yang, D. B. *J. Am. Chem. Soc.* **1980**, *102*, 1028.
(35) Dedieu, A.; Nakamura, S. *Nouv. J. Chim.* **1984**, *8*, 317.
(36) Nakamura, S.; Dedieu, A. *Theor. Chim. Acta* **1982**, *61*, 587.
(37) (a) Laine, R. M. *J. Am. Chem. Soc.* **1978**, *100*, 6451. (b) Alper, H.; Hashem, K. E. *J. Am. Chem. Soc.* **1981**, *103*, 6514. (c) Cann, K.; Cole, W.; Slegeir, W.; Pettit, R. *J. Am. Chem. Soc.* **1978**, *100*, 3969.
(38) Pearson, R. G.; Mauermann, H. *J. Am. Chem. Soc.* **1982**, *104*, 500.
(39) (a) Harkness, A. C.; Halpern, J. *J. Am. Chem. Soc.* **1961**, *83*, 1258. (b) Bercaw, J. E.; Goh, L.-V.; Halpern, J. *J. Am. Chem. Soc.* **1972**, *94*, 6534. (c) Darensbourg, D. *Isr. J. Chem.* **1977**, *15*, 247.
(40) Trautman, R. J.; Gross, D. C.; Ford, P. C. *J. Am. Chem. Soc.* **1985**, *107*, 2355.
(41) King, A. D.; King, R. B.; Yang, D. B. *J. Am. Chem. Soc.* **1981**, *103*, 2699.
(42) Slegeir, W. A. R.; Sapienza, R. S.; Rayford, R.; Lam, L. *Organometallics* **1982**, *1*, 1728.
(43) Weiller, B. H.; Liu, J.-P.; Grant, E. R. *J. Am. Chem. Soc.* **1985**, *107*, 1595.
(44) Ungváry, F. *Coord. Chem. Rev.* **1997**, *160*, 129.
(45) (a) Rubene, N. A.; Davydon, A. A.; Kravstov, A. V.; Ursheva, N. V.; Smol'yaninov, S. I. *Kinet. Catal. (Engl. Transl.)* **1976**, *17*, 400. (b) Tamaru, K. *Dynamic Heterogeneous Catalysis*; Academic Press: New York, 1978; p 121.

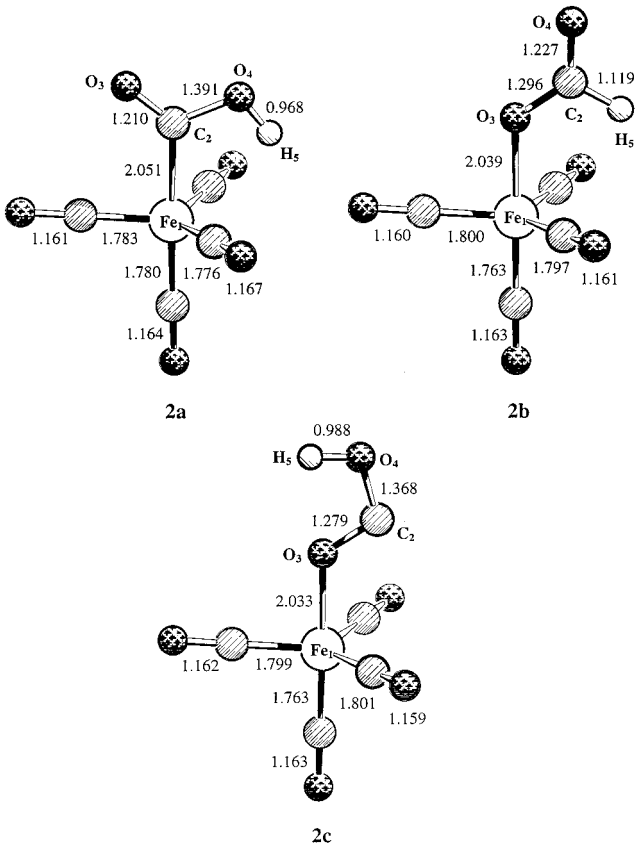

Figure 1. Optimized geometries of the metallocarboxylic acid **2a**, the metalloformate complex **2b**, and the intermediate species **2c** connecting the two former isomers. Bond lengths are in Å.

catalytic reactions of carbon oxides, their intermediacy had already been observed in a number of catalysis-related reactions,[47] as well as on the heterogeneous WGSR.[45] Prompted by these results, we have explored the possibility that a formate intermediate could also take part in the reaction besides the acid **2a**. We have found that the optimized molecular structure of the formate complex $(CO)_4FeO_2CH^-$ corresponds to a real minimum on the potential energy surface (PES). Surprisingly, it turns out to be *more* stable than its isomer, the metallocarboxylic acid, by 5.0 kcal mol^{-1} (Table 1). It means that, from a thermochemical point of view, the observed intermediate should not be the carboxylic acid **2a** but rather the metalloformate complex **2b**. Since the formate anion **2b** has not been observed, the interconversion between the two isomers must be expected to have a high energy barrier so that the carboxylic species derived from the nucleophilic addition, **2a**, cannot undergo isomerization into the more stable form, **2b**.

To confirm the above hypothesis we studied the kinetics for the isomerization reaction **2a** ↔ **2b**. A linear transit was performed in order to locate the TS between the two isomers. It is found that the reaction does not proceed in a single step but in two steps. First, intermediate **2a** (Figure 1) undergoes a 1,2-shift in the acetyl ligand. Such a shift leads to intermediate **2c** depicted in Figure 1. In the second step, the hydrogen atom is transferred from O_4 in **2c** to the vicinal atom C_2 in **2b** through an out-of-plane migration that is likely to involve a sterically impeded three-membered ring in the corresponding TS. Species **2c** is computed to be highly unstable (36.7 kcal mol^{-1} above **2a** and 40.1 kcal mol^{-1} above **2b**). Alternative routes explored for the transformation **2a** ↔ **2b** led to intermediates even energetically higher than **2c**. The lowest energy path connecting **2a** and **2b** involves intermediate **2c**. At least *two* TSs must exist for the conversion between **2a** and **2b** because **2c** shows no imaginary frequencies. No TSs for the reactions **2a** → **2c** → **2b** were located. However, the high energy of intermediate **2c** is enough to prevent interconversion of the two isomers under reaction conditions.

The most accepted mechanism for thermal catalysis[41] of the WGSR by group 6 metal carbonyls has been postulated to proceed via a metallocarboxylic acid intermediate (analogous to **2a**) generated by OH^- attack at a coordinated CO. Although it has been suggested that this is the predominant pathway for thermal catalysis, it is known that photochemical initiation[43] biases the system toward the formate mechanism.[48] In light of our calculations, a similar conclusion can be drawn for the $Fe(CO)_5$-catalyzed WGSR: under mild reaction conditions, the intermediate actually formed is the carboxylic acid **2a**, even though this is not the most stable isomer. The present calculations show that isomerization of the acid into the formate is kinetically prevented. The high energy barriers (above 40 kcal mol^{-1}) could be only surmounted if photochemical conditions were applied (i.e., by irradiating the sample).

Our calculations are also in line with the experimental work of Darensbourg and Rokicki,[48] who found that the anionic species $M(CO)_5COOH^-$ (M = Cr, Mo, W) are less stable than their metalloformate analogues. The relative stabilities of M(COOH) and $M(O_2CH)$ complexes are highly dependent on the nature of the metal center M. For example, PtO_2CH complexes undergo decarboxylation to provide PtH + CO_2 much more readily than their PtCOOH analogues.[49,50] ^{13}C-labeling experiments for the chromium triad also demonstrated that the intermediate afforded from OH^- addition to $M(CO)_6$, $M(CO)_5COOH^-$, and its structural isomer, $M(CO)_5O_2CH^-$, do not interconvert intramolecularly, but only through the intermediacy of a metal pentacarbonyl hydride anion.[48]

3. Decarboxylation. The experimentally reported enthalpy[18] for reaction 3 (-4 ± 7 kcal mol^{-1}) suggests that the reaction is close to thermoneutral, but the error range of the experimental value is rather high. The calculated enthalpies (Table 1) indicate an exothermic reaction. Three different proposals have been made so far for the decarboxylation of $(CO)_4FeCOOH^-$ (Scheme 3). The mechanism illustrated in path A involves addition of OH^- to the hydroxycarbonyl group[40] to give a $C(OH)_2O$ function that subsequently decomposes via loss of HCO_3^-. A second proposal is that the reaction

(46) Darensbourg, D. J.; Rokicki, A.; Darensbourg, M. Y. *J. Am. Chem. Soc.* **1981**, *103*, 3223.

(47) (a) Haynes, P.; Slaugh, L. H.; Kohnle, J. F. *Tetrahedron Lett.* **1970**, 365. (b) Hofman, K.; Schibsted, H. *Chem. Ber.* **1918**, *51*, 1389, 1398. (c) Storch, H.; Golumbic, N.; Anderson, R. B. *The Fischer–Tropsch and Related Syntheses*; Wiley: New York, 1951.

(48) Darensbourg, D. J.; Rokicki, A. *Organometallics* **1982**, *1*, 1685.

(49) Arnold, D. P.; Bennett, M. A. *J. Organomet. Chem.* **1980**, *199*, C17.

(50) Catellani, M.; Halpern, J. *Inorg. Chem.* **1980**, *19*, 566.

Scheme 3. Different Mechanistic Proposals for the Decarboxylation of $(CO)_4FeCOOH^-$

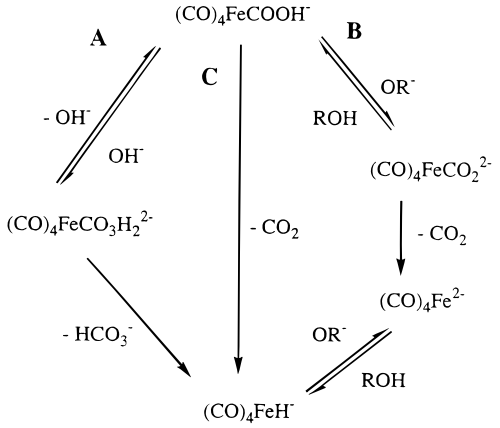

proceeds via a deprotonation mechanism (path B).[38,51] Reports on the relative stability of anionic metal CO_2 complexes, compared to the hydroxycarbonyl analogue,[50,52] led to the conclusion that decarboxylation occurs via a third mechanism (path C) which involves β-elimination of M−H from the M−CO_2H functionality. The latter proposal is the most accepted, especially after the work by Pettit and co-workers,[10] where a concerted elimination of CO_2 was suggested for the reaction rather than loss of CO_2 via a metallocarboxylic anion. Both mechanisms have been proposed for other systems in which decarboxylation of metallocarboxylic acids is inferred.[53] No theoretical studies have been reported yet to support such a concerted mechanism.

Here we present the optimized geometry for the TS that connects **2a** and **3** (Figure 2). The molecular structure of **3** is also given. As can be seen by inspection of the four-centered TS(**2a** → **3**), elimination of CO_2 and formation of the metal hydride occur simultaneously. At the TS the Fe−C and O−H bonds are partially broken (2.051 and 0.968 Å, respectively, in **2a** vs 2.215 and 1.442 Å in the TS), whereas the Fe−H bond is partially formed (2.637 Å in **2a**, 1.693 Å in the TS, and 1.531 Å in **3**). Also, the C_2−O_4 bond (1.281 Å), a single bond in **2a** (1.391 Å), has partially acquired double bond character as in free CO_2 (1.169 Å). Likewise, the $\angle O_3$−C_2−O_4 angle in the TS (133.5°) is about halfway between **2a** (116.6°) and CO_2.

Species **3** (Figure 2) possesses a C_s structure with the hydride ligand occupying an axial position. The Fe−C distance for the three equatorial CO ligands is 1.762 Å whereas the Fe−C bond for the apical CO is slightly longer (1.773 Å) as a result of the large trans influence of hydride (which is a better σ donor than CO). A structure analogous to **3** with H^- occupying an equatorial position has been also computed; we find that such a minimum lies 6.8 kcal mol^{-1} above **3**.

The decarboxylation reaction of the hydroxycarbonyl complex **2a** bears some resemblance to the decarboxylation reaction of formic acid, HCOOH, owing to the

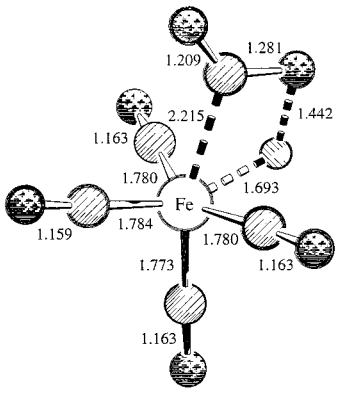

TS(2a→3)

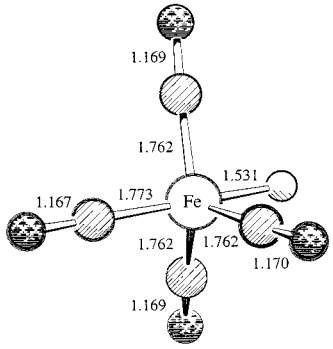

3

Figure 2. Optimized geometries of TS(**2a** → **3**) and intermediate **3**. Bond lengths are in Å.

isolobal analogy[54] between $(CO)_4Fe^-$ and H. It has been shown that the HCOOH decarboxylation reaction, which has a rather high energy barrier in the gas phase, is facilitated by the mediation of water, which enters the TS and acts as a proton relay.[55] The structure of the TS is therefore changed from a four-membered ring to a less energy demanding six-membered ring. These facts suggest that the decarboxylation of **2a** could be *also* water-mediated instead of proceeding as formulated above. The assistance of a base bearing a hydrogen atom has been already invoked as a possible reaction pathway in solution.[40,50,38] To test whether decarboxylation can be catalyzed by a neutral base in the gas phase as well, Lane and Squires[56] have recently examined the reaction of $(CO)_4FeCOOH^-$ with NH_3. No measurable shift in the threshold for decarboxylation was observed with NH_3 as the target gas, indicating that NH_3 *does not lower* the barrier for loss of CO_2 in the gas phase.[56] Also, $(CO)_4FeCOOD^-$ was found not to exchange with NH_3 during decarboxylation to form $(CO)_4FeH^-$, as would be expected if base catalysis involved a concerted 6-center reaction.[56,57] Consequently, it follows that the reaction must occur through a four-membered TS, like TS(**2a** → **3**) reported here. The experimental barrier is slightly overestimated (Table 2), but the geometrical analysis clearly shows that decarboxylation of **2a** proceeds via a

(51) (a) Bercaw, J. E.; Goh, L. Y.; Halpern, J. *J. Am. Chem. Soc.* **1972**, *94*, 6534. (b) Darensbourg, D. J.; Froelich, J. A. *Inorg. Chem.* **1978**, *17*, 3300. (c) Sweet, J. R.; Graham, W. A. G. *Organometallics* **1982**, *1*, 982.

(52) Clark, H. C.; Jacobs, W. J. *Inorg. Chem.* **1970**, *9*, 1229.

(53) (a) Kruck, T.; Hofler, M.; Noack, M. *Chem. Ber.* **1966**, *99*, 1153. (b) Clark, H. C.; Dixon, K. R.; Jacobs, W. J. *J. Am. Chem. Soc.* **1969**, *91*, 1346.

(54) Hoffmann, R. *Angew. Chem., Int. Ed. Engl.* **1982**, *21*, 711.

(55) (a) Ruelle, P.; Kesselring, U. W.; Hô Nam-Tran *J. Am. Chem. Soc.* **1986**, *108*, 371. (b) Ruelle, P. *J. Am. Chem. Soc.* **1987**, *109*, 1722.

(56) Lane, K. R.; Squires, R. R. *J. Am. Chem. Soc.* **1986**, *108*, 7187.

(57) Lane, K. R.; Sallans, L.; Squires, R. R. *J. Am. Chem. Soc.* **1986**, *108*, 4368.

concerted mechanism. It involves rearrangement of the acetyl ligand with a moderate activation barrier through the 4-centered TS depicted in Figure 2.

4. Proton Transfer. Next we investigate the proton transfer from water to the metal hydride **3**, eq 4, to yield dihydride **5** and OH^- (Scheme 2). Dihydride **5**, $(CO)_4FeH_2$, can be regarded as the conjugate acid of **3**. The acidity of **5** in the gas phase has been determined only recently.[58] It was found that $(CO)_4FeH_2$ is an extremely strong acid ($\Delta H_{acid,298}$ $[(CO_4)FeH_2] = 319 \pm 5$ kcal mol^{-1}),[58] comparable in acidity to HBr and HI. This is consistent with the high endothermicity reported in another gas-phase study[18] (71.5 kcal mol^{-1}) for reaction 4. Strong gas-phase acidities are common for organometallic hydrides because of the weak metal−hydrogen bonds.[58,59]

Our calculations are consistent with the experimentally reported acidity[58] of **5** and also with the endothermicity[18] of eq 4. The theoretical acidity of $(CO)_4FeH_2$ computed at CCSD(T) level is 327.6 kcal mol^{-1} (321.7 kcal mol^{-1} after adding the ZPE correction, and 315.7 kcal mol^{-1} when thermal corrections are also included). The theoretical energetics of eq 4, Table 1, are 70.3 and 66.6 kcal mol^{-1} at B3LYP/II++ and CCSD(T)/II++, respectively, also in rather good agreement with the experimental estimate.[18] In addition, the conversion from **3** to **5** (more specific, from **4** to **5**) is the most endothermic step of the whole catalytic cycle (Table 1). This is again in excellent agreement with the recent gas-phase ion study by Sunderlin and Squires,[18] where it was suggested that the highest endothermical step should correspond to reaction 4. Further insight into the energetics of eq 4 can be obtained computationally by splitting the reaction in two processes (Table 1): (i) addition of H_2O to **3** and (ii) elimination of OH^-. Step i leads to the formation of adduct **4** (Figure 3) and is slightly exothermic (Table 1). The actual bottleneck corresponds to step ii. The large endothermicity of the reaction **4** → **5** should be seen in the context of the overall reaction, which is still exothermic after the formation of **5** because the initial steps are highly exothermic.

A charge analysis based on the NBO partitioning scheme has been performed to explain why the water molecule adopts the configuration shown in Figure 3. The primary interaction in adduct **4** takes place between one of the water hydrogens (H_2 in Figure 3) and the oxygen of one of the equatorial CO ligands (H_2-O_2 = 2.258 Å, whereas H_1-O_1 = 3.130 Å). By symmetry, another minimum with the same energy exists involving a H_1-O_1 interaction, where H_1-O_1 = 2.258 Å and H_2-O_2 = 3.130 Å. The iron atom carries a significant negative charge (−0.57 e), whereas the hydride atom is only slightly negative (−0.05 e). It is not surprising, then, that H_1 points toward Fe ($Fe-H_1$ = 3.294 Å). To better accommodate the incoming hydrogen H_1 as the second hydride ligand in **5**, the $\angle C_1-Fe-C_2$ bond angle in **4** is slightly larger (120.0°) than both $\angle C_1-Fe-C_3$ and $\angle C_2-Fe-C_3$ bond angles (115.6 and 117.3°, respectively). At this early stage the proton transfer from H_2O to Fe is not relevant enough yet to differentiate between the two O−H bonds, which still have nearly the same length.

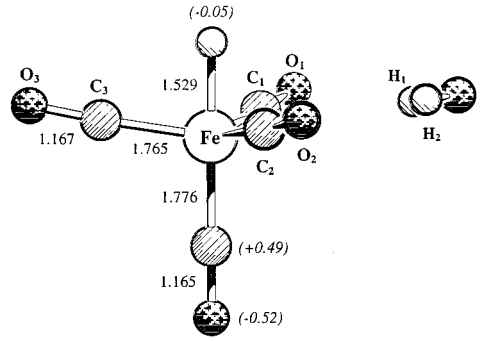

4

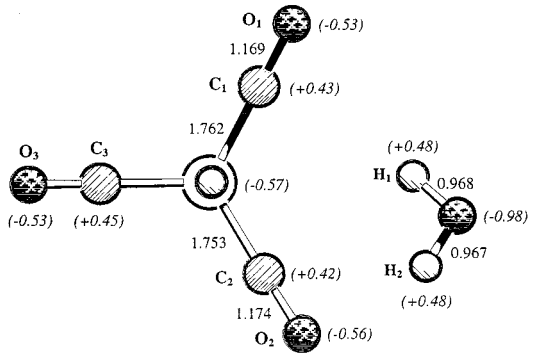

4

Figure 3. Side view (above) and upper view (below) of the optimized geometry of adduct **4**. Bond lengths are in Å and partial atomic charges (in brackets) in a.u.

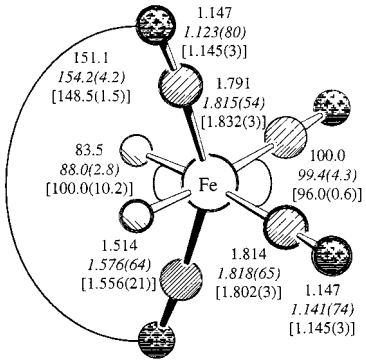

5

Figure 4. Calculated geometrical parameters of tetracarbonyldihydroiron, **5**. Experimental values from the recent microwave work in ref 62b are given in italics. Experimental values from the previous gas-phase electron diffraction study in ref 62a are given in square brackets. Bond lengths are in Å and bond angles in degrees.

Figure 4 shows the optimized molecular structure of $(CO)_4FeH_2$ together with the geometrical parameters experimentally reported[60] for this species. Theories

(58) Miller, A. E. S.; Beauchamp, J. L. *J. Am. Chem. Soc.* **1991**, *113*, 8765.

(59) Pearson, R. G. *Chem. Rev.* **1985**, *85*, 41.

(60) (a) McNeil, E. A.; Scholer, F. R. *J. Am. Chem. Soc.* **1977**, *99*, 6243. (b) Drouin, B. J.; Kukolich, S. G. *J. Am. Chem. Soc.* **1998**, *120*, 6774.

based on electronic arguments[61] predict that, in dihydrides of the type L_4FeH_2, the FeL_4 core should show distortion toward the tetrahedral limit since the H^- ligand is a good σ donor. The theoretical arrangement of carbonyl ligands around Fe (Figure 4) fits excellently the experimentally reported structures, the calculated $\angle C-Fe-C$ angles being within the experimental range of values provided by microwave spectroscopy.[60b]

Two points, however, deserve additional discussion. The first point concerns the exact location of the hydrogen atoms. In $(CO)_4FeH_2$ the calculations predict a H−H distance of 2.016 Å, with $\angle H-Fe-H = 83.5°$ and a short Fe−H bond (1.514 Å), whereas experimental evidence[60] indicates that the two hydrogens should be slightly more separated (2.384 Å according to ref 60a and 2.189 Å according to ref 60b). Hydrogen atom coordinates are often poorly determined using X-ray diffraction, and the X-ray structure alone is not usually considered to give a reliable identification of dihydrogen complexes.[60b] This is reflected by the large range of error (±10.2°) in the work by McNeil and Scholer.[60a] In the work by Drouin and Kukolich,[60b] a more accurate bond angle is reported.

The second point of discussion is the relative order of $Fe-C_{ax}$ and $Fe-C_{eq}$ distances. On the basis of the relative σ-donor abilities of H^- and CO, one would expect the $Fe-C_{eq}$ distance to be longer than the $Fe-C_{ax}$ distance, as theoretically predicted ($Fe-C_{eq} = 1.814$ Å > $Fe-C_{ax} = 1.791$ Å here, and $Fe-C_{eq} = 1.791$ Å > $Fe-C_{ax} = 1.782$ Å in ref 60b). Experimental values from the pioneering study[60a] show the opposite trend (Figure 4). In the more recent study based on microwave spectroscopy,[60b] $Fe-C_{eq}$ and $Fe-C_{ax}$ distances are nearly indistinguishable within the experimental error, but are still in the direction $Fe-C_{eq} < Fe-C_{ax}$. In light of these facts, we encourage experimentalists to reinvestigate this species in more detail.

5. Dihydride vs Dihydrogen Species. Another aspect related to species **5** is the intermediacy of its isomer **6** in the catalytic cycle. Figure 5 shows the optimized geometry of **6**. The short H−H distance (0.894 Å) indicates that such a species is not dihydride **5** but actually the isomer containing H_2. Typical hydrogen atom separation for dihydrogen complexes is ca. 0.8 Å, very close to the free H_2 value of 0.74 Å. As seen from Figure 5, molecular hydrogen lies in the equatorial plane of the metal complex and is linked to Fe through a weak σ bond. The relative order of the $Fe-C_{ax}/Fe-C_{eq}$ distances in **6** (1.818 Å > 1.794 Å) is opposite to that in **5** (1.791 Å < 1.814 Å). This can be rationalized with the large trans influence of H^- in **5** which is not present in **6**. Hydride is a powerful σ donor, whereas H_2 is only a weakly bonded ligand. The enhanced back-donation from Fe to the CO ligands trans to H_2 in **6** results in a shorter $Fe-C_{eq}$ bond length.

According to eq 5, $(CO)_4FeH_2$ decomposes into H_2 and $Fe(CO)_4$. Up to now the species believed to undergo H_2 decomposition in the catalyzed reaction has been always assumed to be isomer **5**. Table 1 reveals that isomers **5** and **6** are very close in energy, the former being more stable by about 8−12 kcal mol^{-1}. Such a difference is low enough to be surmounted under reaction conditions, and therefore, an equilibrium between the two isomers

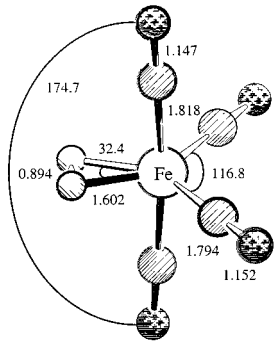

6

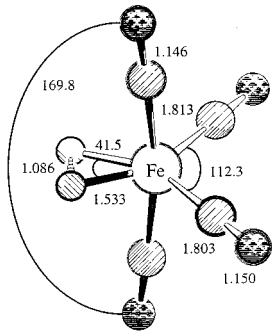

TS(5→6)

Figure 5. Optimized geometries for the molecular hydrogen complex **6** and the TS connecting isomers **5** and **6**. Bond distances are in Å and bond angles in degrees.

should be expected to take place provided kinetics do not prevent it. As seen from the TS in Figure 5, the isomerization reaction **5** → **6** proceeds via a smooth rearrangement. It only involves a slight bending of the axial CO ligands, together with opening of the $\angle C_{eq}-Fe-C_{eq}$ angle, and strengthening of the bond between the two hydrogens as well. The eigenvector associated to the unique imaginary frequency ($\nu = 735i$ cm^{-1}) is mainly related to the H−H stretching mode. As expected from the Hammond postulate and the relative energies of **5** and **6**, TS(**5** → **6**) is productlike, and its structure ressembles **6** rather than **5**. Table 2 shows that the activation barrier to reach TS(**5** → **6**) is also very low or quasi-inexistent. In consequence, the interconversion between the two isomers is feasible both thermodynamically and kinetically, and the two species may exist and participate in the catalytic cycle.

To our knowledge, this is the first time that the molecular configuration of η^2-dihydrogen iron tetracarbonyl **6** has been reported. No previous structural data exist in the literature for such a complex although there is now indirect evidence for its existence.[60b] Our findings confirm a very recent study on the PES of the H−Fe−H symmetric bend in the dihydride $(CO)_4FeH_2$,[60b] where it was shown that, at an angle of 27°, the two H atoms approach to approximately the distance of a molecular hydrogen bond. Moreover, at that angle, there is a local minimum in energy which lies 3000 cm^{-1} above the dihydride, which is the ground state. Although the authors do not report any structure for such a local minimum, they point out that it would correspond to a "dihydrogen" complex,[60b] which is in excellent agreement with our results for species **6**. Their global

(61) Elian, M.; Hoffmann, R. *Inorg. Chem.* **1975**, *14*, 1058.

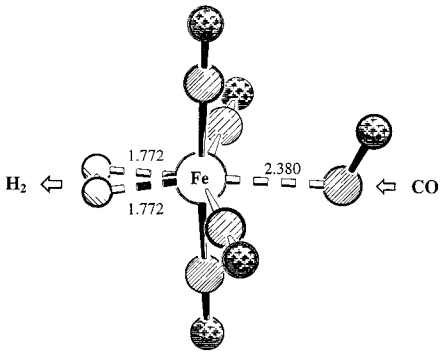

Figure 6. Molecular structure of the upperbound for the new TM-containing S_N2-type associative/dissociative mechanism formulated for the path connecting species **6** and **1**. Selected distances are in Å.

minimum, a "classical dihydride", would correspond to our species **5**.

6. The Last Stages of the Reaction. The classically assumed reaction path from $(CO)_4FeH_2$ to $Fe(CO)_5$ (Scheme 1) involves reductive elimination of H_2 and addition of CO. A logical mechanistic sequence for metal complexes is, first, the reductive elimination of H_2 (eq 5) followed by CO addition to $Fe(CO)_4$ (eq 6). This notwithstanding, contradictory arguments exist for and against reactions 5 and 6 being the last steps in the catalytic cycle.[38,62−64]

Preliminary rate studies with an alkaline solution, ruthenium-based catalyst, indicated a first-order rate dependence on P_{CO}.[65] Since CO addition to an unsaturated complex, eq 6, seems an unlikely rate-limiting step for this cycle, the classically assumed mechanism may not fit the reported evidence.[65] Experiments instead suggest that an alternative pathway should exist where CO is in fact participating in a rate-limiting dihydrogen elimination pathway. No alternative paths, however, have been explored so far in an attempt to find a mechanism fully consistent with the experimental data.[65]

Here we explored a mechanistic proposal that would take into account the above-mentioned participation of CO during H_2 elimination (Scheme 2). A possible way to fulfill this requirement is through an S_N2-type mechanism which involves approach of CO to $(CO)_4FeH_2$ from the side opposite to H_2, and simultaneous ejection of H_2 (Figure 6). Such a mechanism is completely unknown in the field of group 8 organotransition metal chemistry, although ubiquitious examples exist in the literature for the analogous S_N2 reaction in organic chemistry.

Unfortunately, the novel proposal involving a TM-containing S_N2-type mechanism was found to have no chances to compete with the classical route. The estimated upper bound derived from the computed linear transit (28.9 kcal mol^{-1} above the separated species) is still larger than the computed enthalpy for the rate-limiting step of the classical path (step **5** → **7** + H_2). All attempts to locate a TS by fully optimizing downhill the upper-bound energy structure failed. Despite its unique imaginary frequency of 126.7*i* cm^{-1}, the upper-bound energy structure decomposes into $Fe(CO)_4 + CO + H_2$. Therefore, it is concluded that the reaction has to proceed through the less-energy-demanding path despite not being fully consistent with the experimental facts.[65]

A possible alternative to the above explored backside S_N2 substitution could be a mechanism proceeding via a frontside nucleophilic substitution on Fe, i.e., via attack of CO through one of the octahedral faces above or below H_2. Such an alternative path, however, does not seem very promising either, although the metal 3d orbitals pointing toward the leaving group H_2 participate significantly in the LUMO of the complex. A recent study[66] on the model reaction system Pd + CH_3Cl has addressed the question if nucleophilic substitution could be competitive in the formation of the oxidative insertion product, CH_3PdCl. It was found that the high endothermicity of the S_N2 process prevented that route from being a competitive alternative to oxidative insertion.[66]

Next we discuss the decomposition of $(CO)_4FeH_2$ into $Fe(CO)_4$ and H_2 according to Scheme 2. The enthalpy of reaction[5] has been measured to be 26 ± 2 kcal mol^{-1} in solution.[38] It has not been specified if such an activation enthalpy corresponds only to the dihydrogen binding energy in $(CO)_4Fe-H_2$ (i.e., to the reaction **6** → **7** + H_2) or if it also includes the dihydride/dihydrogen isomerization energy (i.e., if it corresponds to the global step **5** → **7** + H_2). Given the small difference in energy between **5** and **6** (Table 1), and the fact that **6** has not been observed yet, it seems reasonable to believe that the reported value corresponds to the decomposition of the more stable isomer, **5**. No data have been reported for reaction **5** → **7** + H_2 in the gas phase. It has been previously assumed[18] that the value of 26 ± 2 kcal mol^{-1} would be also applicable to the gas phase, noting that the gas-phase and solution enthalpies of activation were essentially identical for an analogous reaction. The calculated enthalpies collected in Table 1 for eq 5 are consistent with the experimental measurements.[38] Dihydride decomposition is computed to be endothermic by ca. 30 kcal mol^{-1}, DFT calculations slightly underestimating the endothermicity.

7. Regeneration of the Starting Catalyst. The final step in the catalytic cycle, eq 6, corresponds to the reverse of the CO dissociation from **1**, a well-known benchmark for first-bond dissociation energies (FBDE) in TM carbonyls chemistry.[29] The calculation of the FBDE for the unsaturated $Fe(CO)_5$, and the molecular/electronic ground-state structure for the unsaturated species $Fe(CO)_4$ has received considerable attention.[67] Experimental investigations indicate that $Fe(CO)_4$ possesses a high-spin C_{2v} ground state.[68−70] The d^8 $Fe(CO)_5$

(62) (a) Brandes, K. H.; Jonassen, H. B. *Z. Anorg. Allg. Chem.* **1966**, *343*, 215. (b) Mark'o, L.; Ungváry, F. *J. Organomet. Chem.* **1969**, *20*, 205. (c) Muetterties, E. L.; Watson, P. L. *J. Am. Chem. Soc.* **1978**, *100*, 6978.

(63) Sweaney, R. L. *J. Am. Chem. Soc.* **1981**, *103*, 2410.

(64) Pearson, R. G. *Trans. Am. Crystallogr. Assoc.* **1978**, *14*, 89.

(65) Ford, P. C.; Rinker, R. G.; Ungermann, C.; Laine, R. M.; Landis, V.; Moya, S. A. *J. Am. Chem. Soc.* **1978**, *100*, 4595.

(66) Bickelhaupt, F. M.; Ziegler, T.; Schleyer, P.v. R. *Organometallics* **1995**, *14*, 2288.

(67) (a) Lionel, T.; Morton, J. R.; Preston, K. F. *J. Chem. Phys.* **1982**, *76*, 234. (b) Bogdan, P.; Weitz, E. *J. Am. Chem. Soc.* **1989**, *111*, 3163. (c) Bogdan, P.; Weitz, E. *J. Am. Chem. Soc.* **1990**, *112*, 639. (d) Lyne, P. D.; Mingos, D. M. P.; Ziegler, T.; Downs, A. J. *Inorg. Chem.* **1993**, *32*, 4785. (e) Decker, S. A.; Klobukowski, M. *J. Am. Chem. Soc.* **1998**, *120*, 9342. (f) González-Blanco, O.; Branchadell, V. *J. Chem. Phys.* **1999**, *110*, 778.

(68) (a) Perutz, R. N.; Turner, J. J. *J. Am. Chem. Soc.* **1975**, *97*, 4791. (b) Davies, B.; McNesh, A.; Poliakoff, M.; Turner, J. J. *J. Am. Chem. Soc.* **1977**, *99*, 7573. (c) Davies, B.; McNesh, A.; Poliakoff, M.; Tranquille, M. Turner, J. J. *Chem. Phys. Lett.* **1978**, *52*, 477.

Table 3. Optimized Geometries for the Coordinatively Unsaturated $Fe(CO)_4$ Species 7 ($^1A_1$) and 7′ ($^3B_2$) with Bond Lengths in Å and Bond Angles in deg

geometrical parameter	this work		ref 73		ref 32	
	$^1A_1$	$^3B_2$	$^1A_1$	$^3B_2$	$^1A_1$	$^3B_2$
$Fe-C_{ax}$	1.815	1.865	1.834	1.859	1.909	1.878
$Fe-C_{eq}$	1.782	1.842	1.793	1.820	1.874	1.884
$C-O_{ax}$	1.150	1.148	1.153	1.156	1.181	1.169
$C-O_{eq}$	1.154	1.150	1.160	1.160	1.177	1.174
$\alpha(C_{ax}-Fe-C_{ax})$	155.4	146.2	167.7	147.4	151	150
$\beta(C_{eq}-Fe-C_{eq})$	130.4	98.3	129.8	99.4	125	104

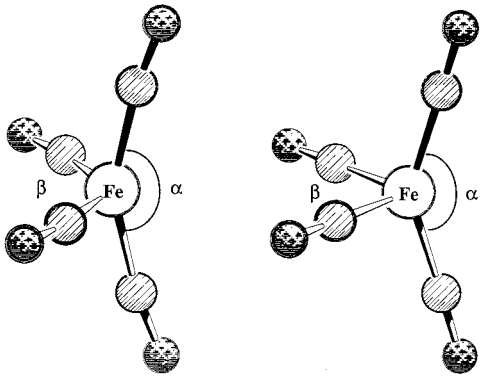

7 7'

Figure 7. Optimized geometries of the $Fe(CO)_4$ species in the electronic states $^1A_1$ (left) and $^3B_2$ (right).

species turns out to correlate to a tetrahedral e^4t^4 $Fe(CO)_4$ configuration which has a triplet ground state and does Jahn−Teller distort to a C_{2v} symmetry.[68,71] Since $Fe(CO)_5$ has the same *A* factor as the group 6 carbonyls, its dissociation has been reported[72] to be spin-allowed, yielding the excited singlet state. The experimentally determined $Fe(CO)_5$ FBDE (41.5 kcal mol^{-1})[72] corresponds therefore to the singlet $Fe(CO)_4$ product.

We have carried out geometry optimization studies on the $Fe(CO)_4$ species within C_{2v} symmetry constraints. Considerations have been given to the $^1A_1$ singlet with a $(3a_2)^2(8b_1)^2(15a_1)^2(9b_2)^2$ configuration as well as to the $^3B_2$ triplet with a $(3a_2)^2(8b_1)^2(15a_1)^2$ $(9b_2)^1(16a_1)^1$ configuration.[61] The optimized geometries are shown in Table 3. The optimized ground state of $Fe(CO)_4$ at the B3LYP/II level is the $^3B_2$ triplet state with a distorted tetrahedral geometry **7′** (Figure 7) in which the $\alpha(C_{ax}-Fe-C_{ax})$ angle is 146.2° and the $\beta(C_{eq}-Fe-C_{eq})$ angle is 98.3° (Table 3). The $^1A_1$ singlet is 8.2 kcal mol^{-1} higher in energy, with the butterfly conformation given by **7**.

Our findings are in good agreement with experimental estimates by Poliakoff et al.[70] Ziegler et al.[73] have also found a triplet ground state for $Fe(CO)_4$ in a previous DFT study; however, these authors reported a singlet−triplet energy splitting[73] of only 1.8 kcal mol^{-1}. A more accurate ab initio study on $Fe(CO)_4$ of Barnes et al.[32] gave a $^3B_2$ triplet ground state for $Fe(CO)_4$ at the MCPF level of theory. They also calculated an approximate structure for the $^1A_1$ singlet state, optimized by an uncoupled variation of each degree of freedom, and reported a splitting[32] of 15 ± 5 kcal mol^{-1}. Our singlet−triplet energy splitting is midway between that of Ziegler et al.[73] and the value computed by Barnes et al.[32] Experimental data are not available for comparison. Very recently, Decker and Klobukowski[67e] have computed the singlet−triplet spacing for $Fe(CO)_4$ using different functionals. Their values range from 3.4 kcal mol^{-1} (BP86) to 12.5 (B3PW91). Hoffmann and coworkers[74] have also explored the lowest energy singlet state, but with a C_{3v} structure, and found it to be 6.7 kcal mol^{-1} above the triplet ground state.

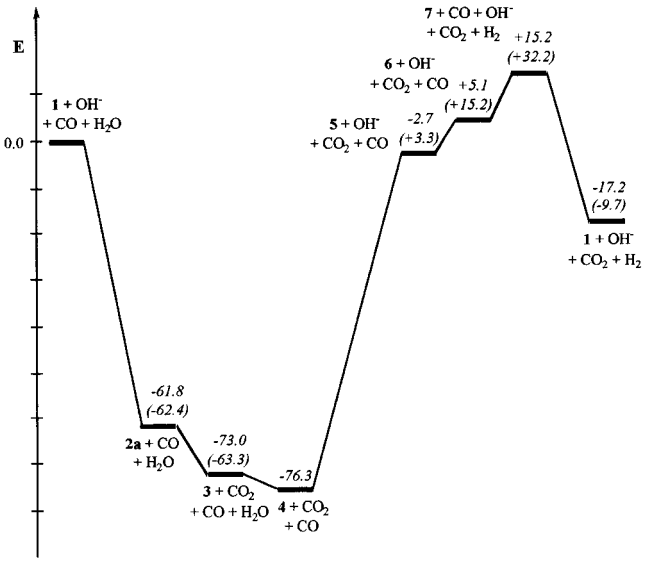

Figure 8. Thermochemical profile for the model $Fe(CO)_5$-catalyzed water gas shift reaction in the gas phase at B3LYP/II++ (enthalpies in kcal mol^{-1}). CCSD(T) values are given in parentheses.

The theoretical enthalpy compiled in Table 1 for reaction 6 at the CCSD(T)/II++ level is in excellent agreement with the experimental estimate.[72] As mentioned above, the latter value has been reported to correspond to the addition of CO to *singlet* $Fe(CO)_4$. The computed value in Table 1 likewise refers to **7** and not to **7′**.

The reaction course is summarized in Figure 8, which shows the thermochemical profile for the model reaction as given by our calculations. As can be seen, even after the very endothermic step **4** → **5**, the overall reaction is energetically still *below* the reactants. The exothermicity of the net reaction is −17.2 kcal mol^{-1} (Table 1). Since formation of **4** from the reactants is *very* exothermic (−76.3 kcal mol^{-1}), the following step can still take place despite being notably endothermic (73.6 kcal mol^{-1}). It should be noted that the activation barrier for the overall reaction is only 15.2 kcal mol^{-1} (formation of **7**). However, some energy has to be added thermally along the way because the intermediates will lose energy via decomposition (loss of CO_2, H_2), and the

(69) Barton, T. J.; Grinter, R.; Thompson, J.; Davies, B.; Poliakoff, M. *J. Chem. Soc., Chem. Commun.* **1977**, 841.
(70) Poliakoff, M.; Weitz, E. *Acc. Chem. Res.* **1987**, *20*, 408.
(71) (a) Burdett, J. K. *J. Chem. Soc., Faraday Trans.* **1974**, *70*, 1599. (b) Nathanson, G.; Gitlin, B.; Rosan, A. M.; Yardley, J. T. *J. Chem. Phys.* **1981**, *74*, 361. (c) Tumas, W.; Gitlin, B.; Rosan, A. M.; Yardley, J. T. *J. Am. Chem. Soc.* **1982**, *104*, 55.
(72) Lewis, K. E.; Golden, D. M.; Smith, G. P. *J. Am. Chem. Soc.* **1984**, *106*, 3905.
(73) Li, J.; Schreckenbach, G.; Ziegler, T. *J. Am. Chem. Soc.* **1995**, *117*, 486.
(74) Radius, U.; Bickelhaupt, F. M.; Ehlers, A. W.; Goldberg, N.; Hoffmann, R. *Inorg. Chem.* **1998**, *37*, 1080.

dissociated particles will take some energy vibrationally, rotationally, and translationally.

Summary and Conclusions

A revision of the $Fe(CO)_5$-catalyzed WGSR in the gas phase has been presented. The main points derived from our study can be summarized as follows.

1. Confirmation of Some of the Previously Assumed Reaction Steps by Providing Theoretical Support to the Experiments. Our calculations lend additional credit to the initial attack of the hydroxyl ion to **1**, and also to the recently accepted decarboxylation of $(CO)_4FeCOOH^-$ via a concerted mechanism involving a 4-centered TS, as well as to the protonation of metal hydride **3**. On the other hand, further revision of the experimentally reported molecular structure of dihydride **5** is claimed.

2. Prediction of New Intermediates both Directly and Indirectly Related to the Catalytic Cycle. Novel species such as **2b**, **2c**, **4** , and **6**, not mentioned in previous studies of the $Fe(CO)_5$-catalyzed WGSR, have been reported for the first time, and their existence/participation in the cycle has been discussed in terms of energies and activation barriers. While adduct **4** and intermediate **6** are shown to take play in the catalytic cycle, species **2b** and **2c** might exist, but probably do not participate in the WGSR. The investigation of the two latter species is relevant for comparison with similar TM complexes reported for group 6.

3. Proposal of Alternative Paths to Some of the Classically Assumed Reaction Steps. In particular, a novel mechanistic hypothesis is suggested and explored for the last stages of the catalytic cycle. Such a route would involve an unprecedented S_N2-type reaction occurring at a TM center; however, it is found to be more energy demanding than the classical route, at least from the upper-bound estimate here reported.

Whether or not the calculations in point 3 have any bearing in reality, it is clear that the present work brings novel data and enlarges the scope for the gas-phase mechanism of the WGSR. Moreover, providing that the new hypotheses can be further confirmed by some direct or indirect evidence, the current results will represent not only valuable information about the $Fe(CO)_5$-catalyzed WGSR but also a new insight in the reactivity of group 8 organometallic compounds. Further research is in progress.

Acknowledgment. This work was supported by Euro-ASCE through a grant under the Training and Mobility of Researchers (TMR) Program, and also by the Deutsche Forschungsgemeinschaft and by the Fonds der Chemischen Industrie. Excellent service by the Centre de Supercomputació de Catalunya is gratefully acknowledged. Additional computer time was given by the HRZ of the Philipps-Universität Marburg and by the HLRS Stuttgart.

Supporting Information Available: Total energies, Cartesian coordinates, harmonic vibrational frequencies, force constants, and IR intensities of all stationary points. This material is available free of charge via the Internet at http://pubs.acs.org.

OM9810504